Data in Brief 21 (2018) 501–510

Contents lists available at ScienceDirect

Data in Brief

journal homepage: www.elsevier.com/locate/dib

Data Article

Dataset of emission and excitation spectra, UV–vis absorption spectra, and XPS spectra of graphitic C_3N_4

Liangrui He [a,1], Mi Fei [a,1], Jie Chen [a], Yunfei Tian [a], Yang Jiang [a], Yang Huang [b], Kai Xu [b], Juntao Hu [b,*], Zhi Zhao [c], Qiuhong Zhang [d], Haiyong Ni [d], Lei Chen [a,e,**]

[a] School of Materials Science and Engineering, Hefei University of Technology, Hefei 230009, China
[b] National Engineering Lab of Special Display Technology, State Key Lab of Advanced Display Technology, Academy of Opto-Electronic Technology, Hefei University of Technology, Hefei 230009, China
[c] Hefei National Laboratory for Physical Sciences at the Microscale, University of Science and Technology of China, Hefei 230026, China
[d] Guangdong Province Key Laboratory of Rare Earth Development and Application, Guangdong Research Institute of Rare Metals, Guangdong Academy of Sciences, Guangzhou 510651, China
[e] Intelligent Manufacturing Institute of Hefei University of Technology, Hefei 230051, China

ARTICLE INFO

Article history:
Received 30 June 2018
Received in revised form
30 August 2018
Accepted 30 September 2018
Available online 3 October 2018

Keywords:
Graphitic C_3N_4
Luminescence spectra
Absorption spectra
X-ray photoelectron spectroscopy (XPS)

ABSTRACT

In this data article, the normalized emission and excitation spectra, the ultraviolet-visible (UV–vis) absorption spectra, and the X-ray photoelectron spectroscopy (XPS) of bulk-powders and nano-structured graphitic C_3N_4 (g-C_3N_4) were presented, which are helpful to get insight into the crystal and electronic structures of g-C_3N_4, especially on determining the energy levels and the mechanisms of luminescence originating from electron transitions. This data article is related to our recent publication (He et al., in press) [1]. The absorption, excitation and emission spectra are vital to illustrate the optoelectronic performances in terms of photoluminescence, photocatalysis,

DOI of original article: https://doi.org/10.1016/j.mattod.2018.06.008
* Corresponding author.
** Corresponding author at: School of Materials Science and Engineering, Hefei University of Technology, Hefei 230009, China.
E-mail addresses: jthu@hfut.edu.cn (J. Hu), shanggan2009@qq.com (L. Chen).
[1] These authors contributed equally as co-first authors.

https://doi.org/10.1016/j.dib.2018.09.123

electroluminescence, etc., from the viewpoint of electron transitions intrinsically.

Specifications table

Subject area	Physics, chemistry, materials science
More specific subject area	Solid-state luminescence in condensed luminescence, solid-state structure in inorganic chemistry, functional materials in photoluminescence, electroluminescence, photocatalyst, etc.
Type of data	figure
How data was acquired	Fluorescence spectrophotometer (F-4600 Hitachi), ultraviolet-visible (UV-VIS) spectroscopy (UV-3600, Shimadzu), X-ray Photoelectron Spectrometer (ESCALAB250Xi, Thermo)
Data format	Raw, analyzed
Experimental factors	Temperatures, reaction atmospheres, bulk-powder or nanostructure
Experimental features	The intensity and wavelength of emission, excitation, and absorption spectra; and the binding energy position and the counts per second in XPS
Data source location	Hefei, China
Data accessibility	Data are provided with this article

Value of the data

- The electron transitions and their corresponding energy levels could be identified from the normalized emission and excitation spectra.
- The fast relaxation of electrons from excited states to the ground state without the Stokes shift radiation could be discriminated by comparing absorption spectra with emission spectra together.
- The XPS data are helpful to reason out the way and reaction process of the thermal condensation of melamine to form g-C_3N_4 and thereby, to illustrate the performances from viewpoint of crystal structure.
- The emission, excitation and absorption spectra of g-C_3N_4 are helpful to recognize its electronic structure.
- The electronic and crystal structures are useful to interpret the intrinsic properties of g-C_3N_4 in terms of photoluminescence, electroluminescence, photocatalysis, etc.

1. Data

The normalized emission spectra of g-C_3N_4 powders synthesized at various temperatures in air and N_2 atmospheres are shown in Fig. 1a,b, respectively, which shows that the emission peaks red-shift with temperature increasing from 450 to 600 °C. The asymmetrical emission band mainly consists of the π^*–Lp (lone pair electrons) and π^*–π transitions. The normalized excitation spectra of g-C_3N_4 powders synthesized at various temperatures in air and N_2 atmospheres are displayed in as Fig. 1c,d, in which the excitation peaks at 339, 375, 399 and 431 nm were attributed to the LP–δ^* (* indicates the antibond), LP–π^*, π–π^*, and traps absorption, respectively.

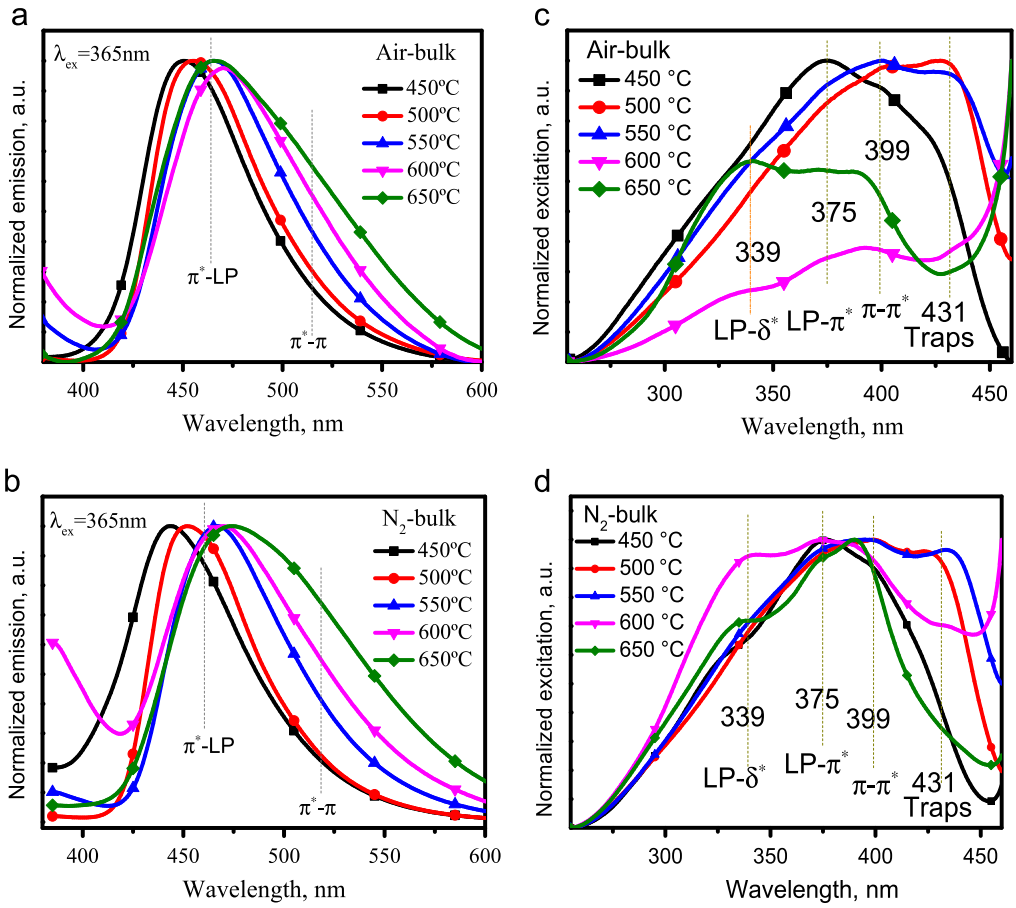

Fig. 1. The normalized emission and excitation spectra of bulk powders synthesized at different temperatures in Air and N_2 atmospheres: a, b, the emission spectra under excitation of 365 nm; c, d, the excitation spectra achieved by monitoring the strongest emission in a,b.

The normalized emission and excitation spectra of g-C_3N_4 quantum dots (QDs) are presented in Fig. 2. After being exfoliated into QDs, the emission and excitation peaks shift towards high energy direction (i.e., blueshift) evidently, as seen by the comparison of Fig. 2a–d with Fig. 1a–d. Besides, the δ*–Lp transition peaked at 405 nm was observed in Fig. 2b for the sample synthesized at 450 °C under N_2 atmosphere, suggesting the electrons cannot relax from the high-energy δ* state to the low-energy π* state efficiently. Maybe, the π orbital is not well formed under the condition of 450 °C in N_2 atmosphere.

The absorption spectra of g-C_3N_4 bulk powders synthesized at various temperatures in air and N_2 atmospheres, respectively, are shown in Fig. 3. Besides the LP–δ*, LP–π*, and π–π*, transitions as correspond to the excitation bands in Fig. 2a, b, one band peaked at about 266 nm was observed in Fig. 3a, b, which was attributed to the charge effect band (i.e., photocurrent, marked with CTB). The CTB was nearly not observed under 450 °C. However, the increase of CTB in intensity with an increase of temperature from 500 to 650 °C suggests that the exorbitant condensation of the g-C_3N_4 easily result in the photocurrent, which can explain the decrease of g-C_3N_4 luminescence upon increasing temperature from 500 to 650 °C. Moreover, the absorption within 440–600 nm increases with temperature increasing from 450 to 650 °C. The position of this absorption band is consistent with the

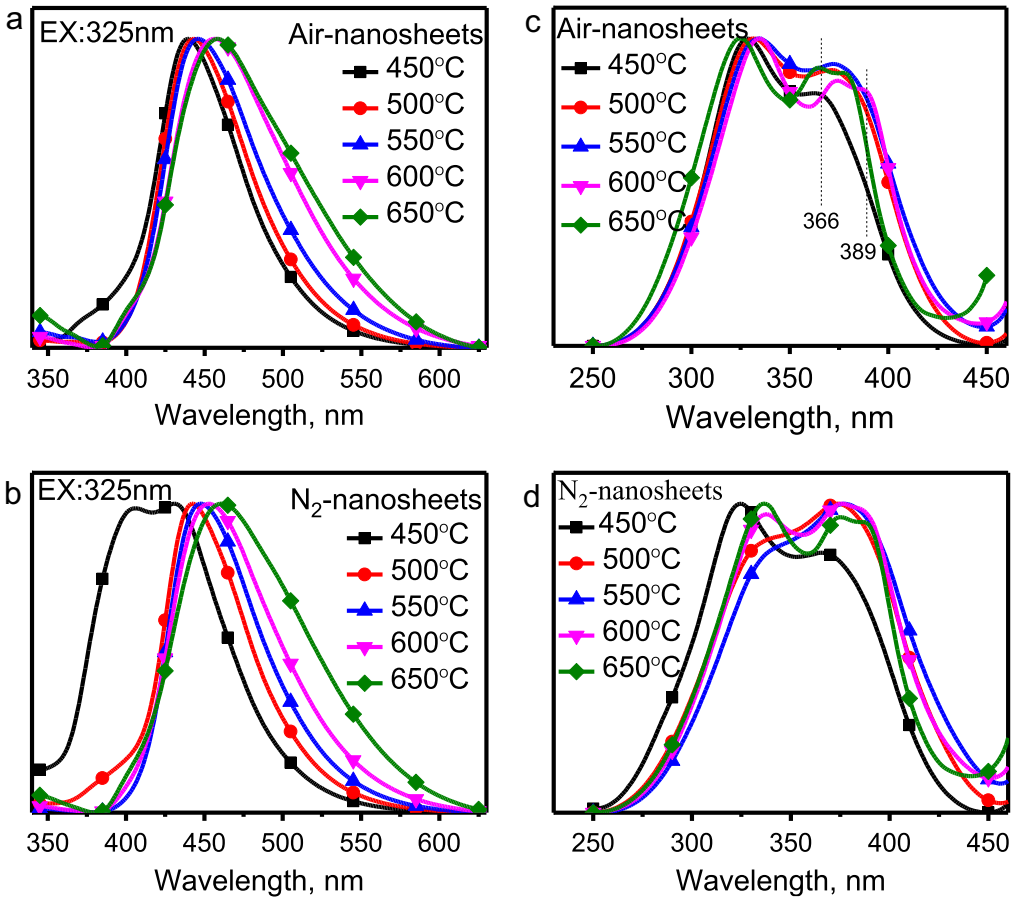

Fig. 2. The normalized emission and excitation spectra of quantum dots achieved by ultrasonic exfoliating the above bulk powders synthesized at different temperatures in Air and N_2 atmospheres, respectively; a, b, the emission excited with 325 nm; c, d, the excitation spectra synthesized in N_2, respectively.

absorption wavelength of traps in Fig. 1c, d. So, it is naturally to assign the absorption band within 440–600 nm to crystal defects. Besides, the absorption within 440–600 nm overlaps with the emission band very well, as comparison of absorption spectra with emission spectrum displayed in Fig. 3a, b. Therefore, the absorption within 440–600 nm is mainly caused by the fast relaxation of electrons from the high-energy excited states to the ground band without the Stokes shift, overlaying with the absorption of crystal traps. After being exfoliated into QDs, the absorption bands of CTB and fast relaxation disappear, as seen from Fig. 3c, d.

The intensity of the LP–π^*, and π–π^* absorptions of g-C_3N_4 QDs in Fig. 3c, d are far weaker over those of bulk powders in Fig. 3a, b, suggesting the π orbital was partially damaged or broken during the process of ultrasonic exfoliating and in turn resulting in electrons cannot relax from high-energy δ^* to low-energy π^* state efficiently. Accordingly, the LP-δ^* transition dominates the absorption of g-C_3N_4 QDs in Fig. 3c, d.

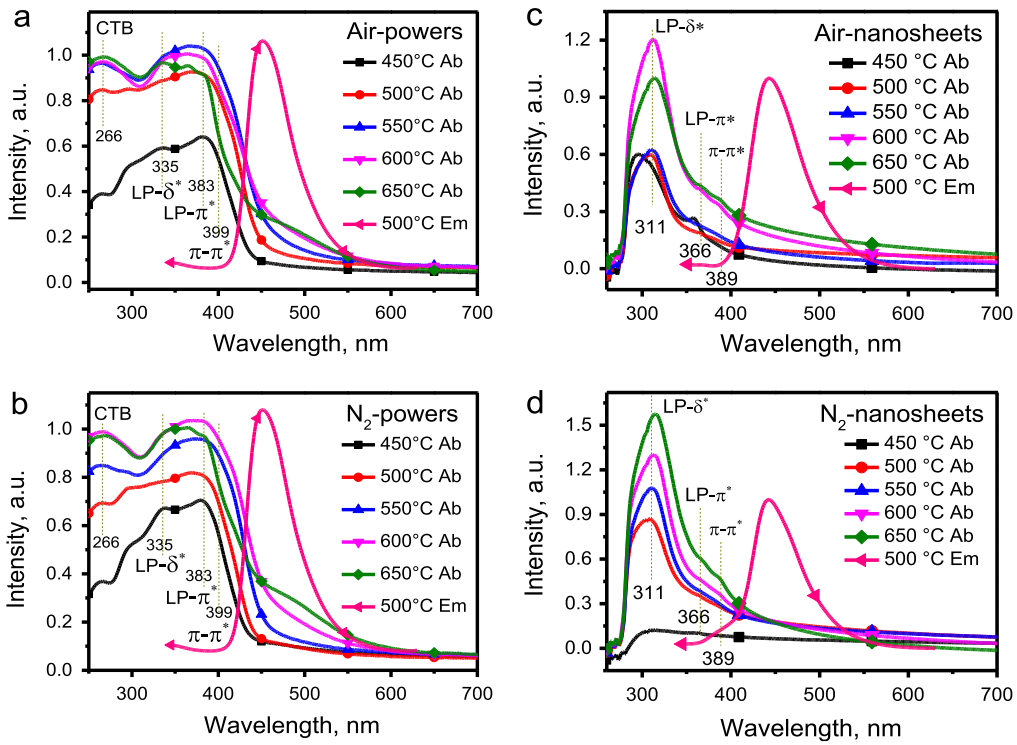

Fig. 3. The comparison of absorption spectra with emission spectra for the bulk powders and quantum dots: a,b, the bulk powders synthesized at variant temperatures in Air and N_2 atmospheres, respectively; c,d, the quantum dots obtained by ultrasonic exfoliating the bulk powders in a,b.

The raw C 1s and N 1s XPS of g-C_3N_4 bulk powders and their fitted spectra by using the XPS PEAK 4.1 program are depicted in Fig. 4 and Fig. 5, respectively. The composition of C, N and O elements for the samples synthesized at various temperature in air and N_2 atmospheres was summarized in Table 1. The analyses on XPS spectra in Figs. 4 and 5 confirm that the structure of g-C_3N_4 consists of basic unit of tri-s-triazine ring, which is connected by the N atoms to form a π–conjugated polymeric network [2–8].

Moreover, the highest ratio of graphitic-to-triazine carbon was observed in the sample synthesized at 500 °C in N_2 atmosphere and the second highest ratio of graphitic-to-triazine carbon was observed in the sample synthesized at 450 °C in air ambient. These ratios are consistent with the strongest and the second strongest luminescence of g-C_3N_4 powders presented in Fig. 2 and Fig. 3, respectively, in Ref. [1], indicating the luminescence efficiency is related with the type of carbon existence closely.

2. Experimental design, materials and methods

The material and methods used to obtain the data of emission and excitation, absorption, and XPS spectra were described in [1]. The emission and excitation spectra of bulk-powders and nano-structured g-C_3N_4 were collected with Hitachi F4600 spectrometer, and the spectra in Figs. 1 and 2

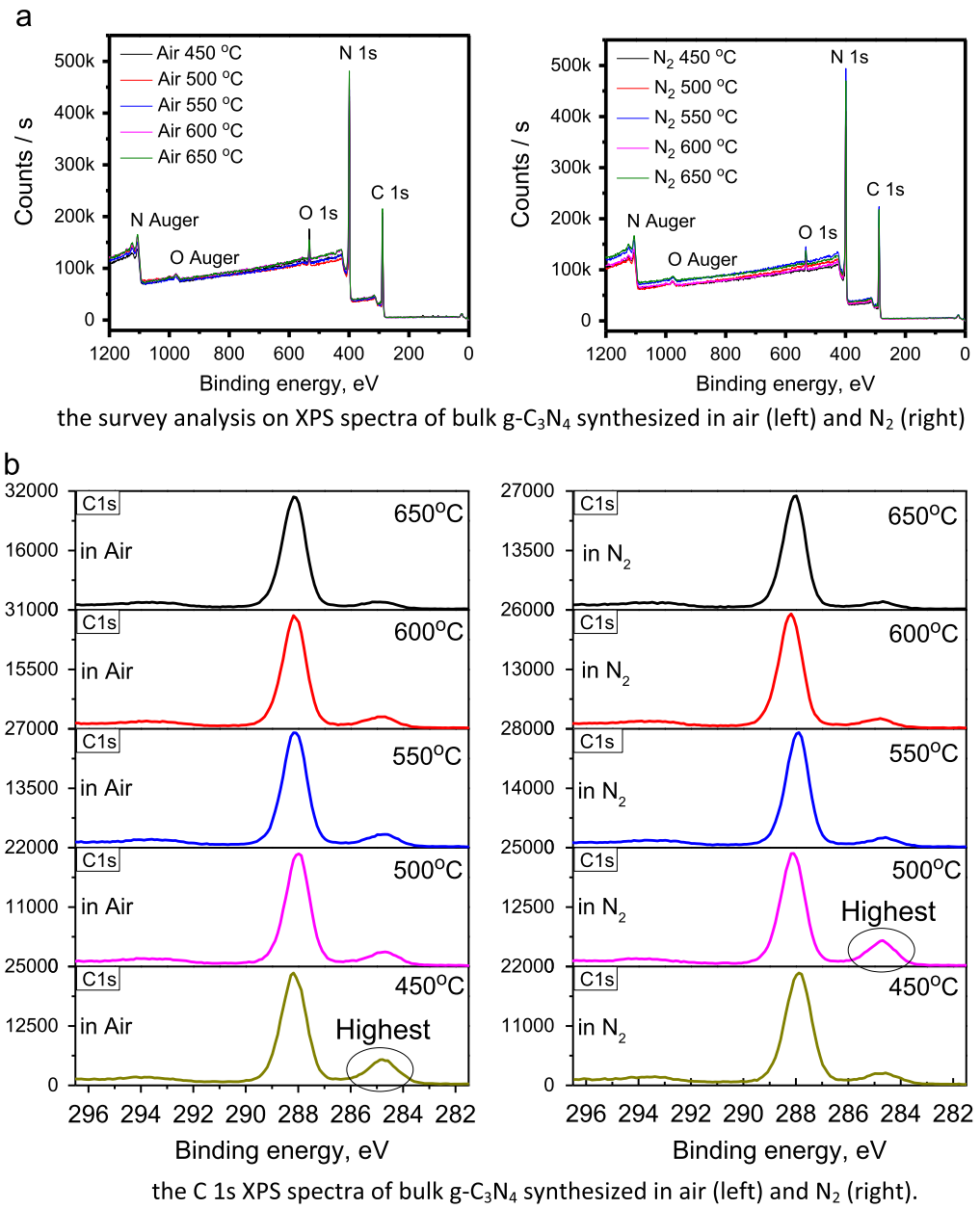

the survey analysis on XPS spectra of bulk g-C_3N_4 synthesized in air (left) and N_2 (right)

the C 1s XPS spectra of bulk g-C_3N_4 synthesized in air (left) and N_2 (right).

Fig. 4. The survey, C 1s, N 1s, and O 1s XPS spectra of bulk g-C_3N_4 powders synthesized at variant temperatures in air and N_2, respectively.

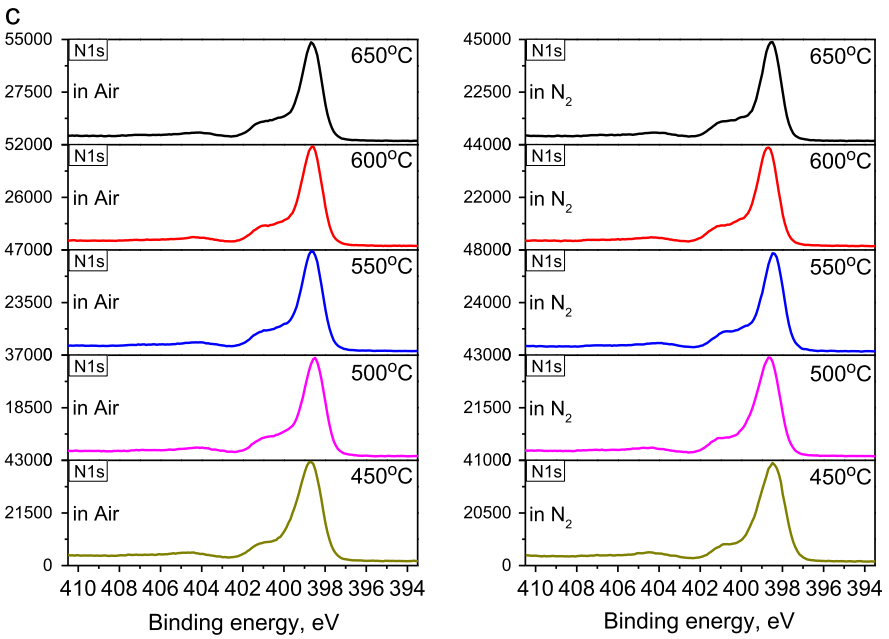

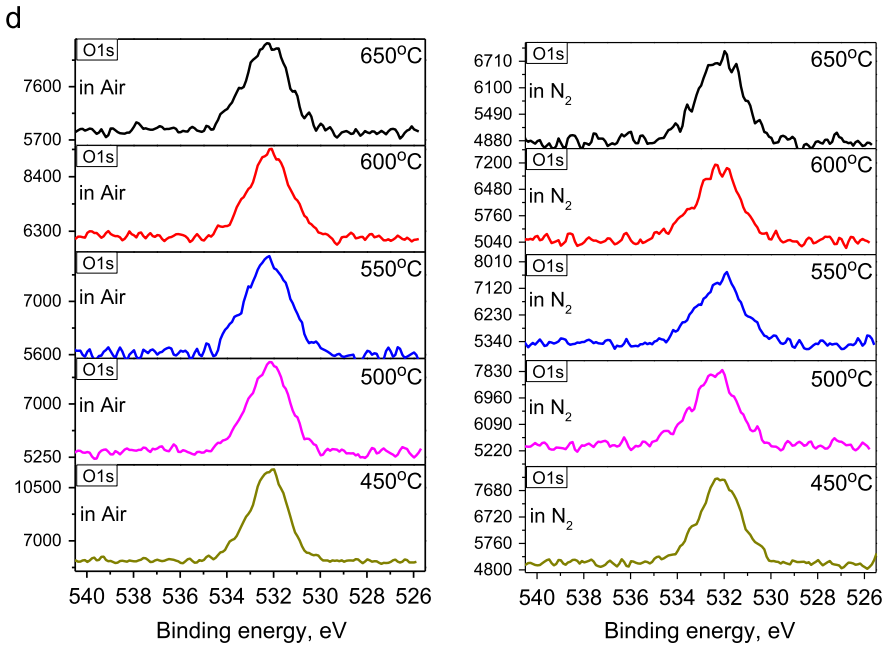

Fig. 4. (*continued*)

were normalized to determine the energy levels. The absorption spectra in Fig. 3, recorded with UV-3600 spectra, were further in comparison with emission spectra to determine electron transition and the mechanisms thereof. The original XPS spectra, including the survey, C 1s, N 1s, and O 1s, of bulk g-C_3N_4 powders, measured with using the Thermo ESCALAB250Xi X-ray Photoelectron Spectrometer, were displayed in Fig. 4. The C 1s and N 1s XPS were fitted by using the XPS PEAK 4.1 program, as shown in Fig. 5, to reveal the way of thermal condensation and chemical bonding.

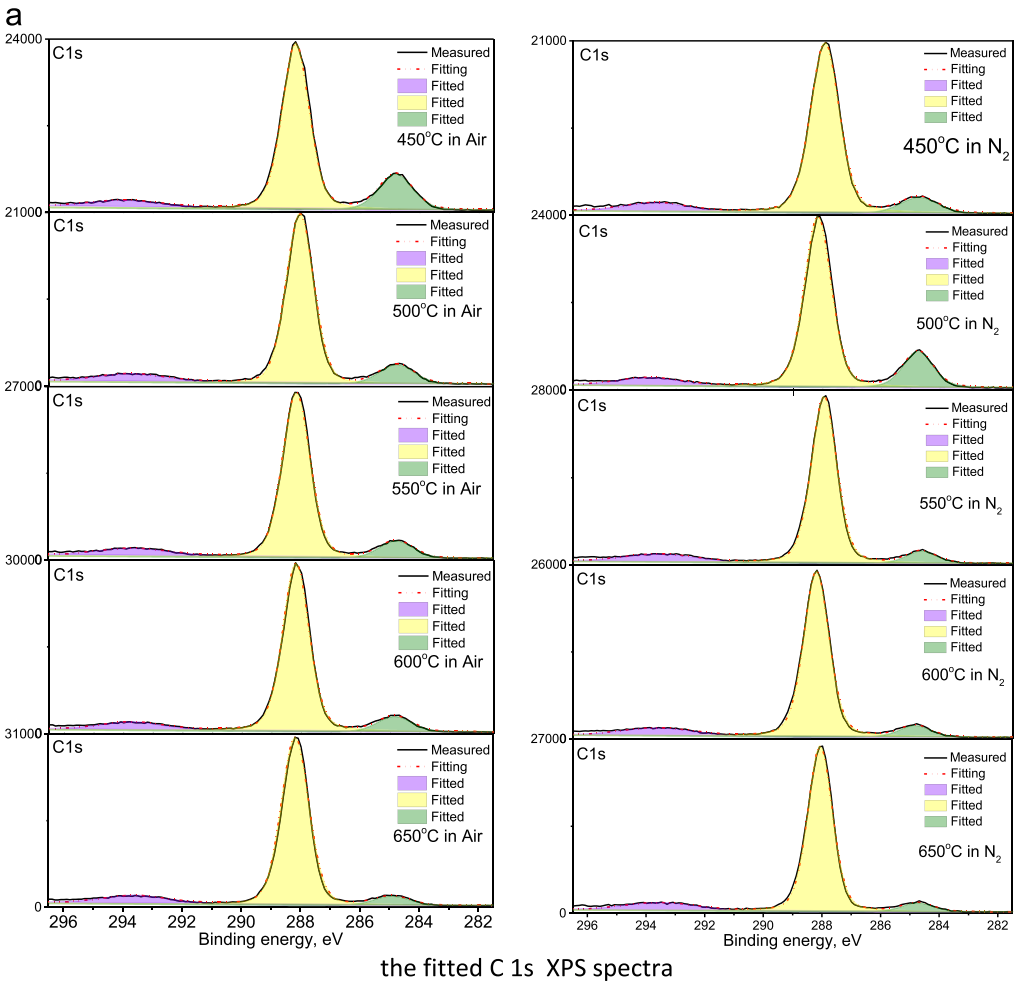

Fig. 5. The fitted C 1s and N 1s XPS spectra, as corresponding to Fig. 4b,c, by using the XPS PEAK 4.1 program, of g-C_3N_4 powders synthesized at variant temperatures in air and N_2, respectively.

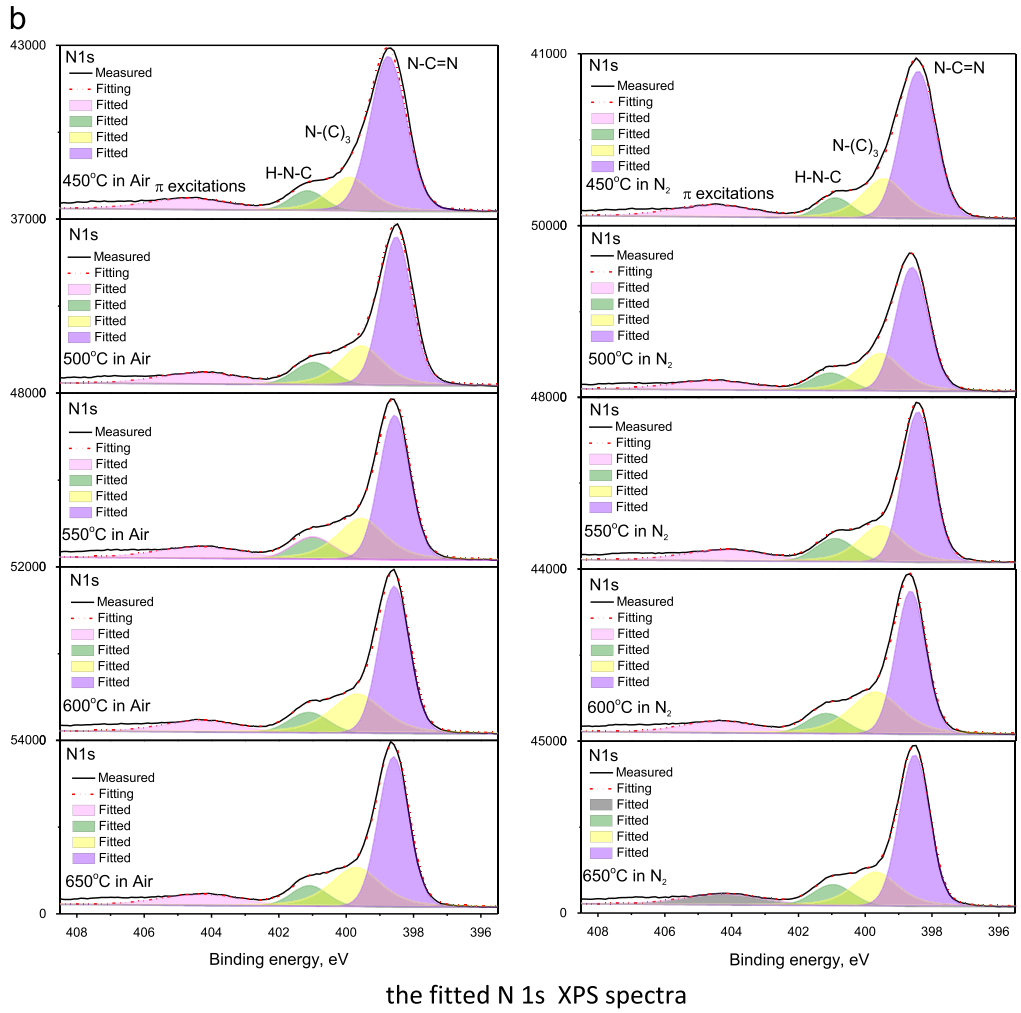

Fig. 5. (*continued*)

Table 1
the percent of C, N and O atoms in bulk g-C_3N_4 powders obtained by fitting the XPS spectra in Fig. 4 by using the XPS PEAK 4.1 program, as corresponding to Fig. 5.

Items	450 °C	500 °C	550 °C	600 °C	650 °C	Conditions
C1s	42.04	42.91	42.14	42.12	41.42	Synthesized in Air
N1s	51.8	52.62	54.01	53.63	54.58	
O1s	6.16	4.47	3.85	4.26	4	
C1s	39.44	43.55	41.81	41.91	41.83	Synthesized in N_2
N1s	55.95	52.78	54.68	54.66	54.45	
O1s	4.61	3.68	3.51	3.43	3.72	

Acknowledgements

This work was supported by the National High-Tech R&D Program (863 program) (2013AA03A114), the National Natural Science Foundation of China (21875058 and U1332133), the Project of Science and Technology of Guangdong Province (2017B090901070) and Project of Science and Technology of Anhui Province (1301022062), the Science and Technology Project of Guangzhou (201604016005), and the Special Fund for Research and Development of the Hefei Institute (IMICZ2015112), China.

Transparency document. Supplementary material

Transparency document associated with this article can be found in the online version at https://doi.org/10.1016/j.dib.2018.09.123.

Appendix A. Supplementary material

Supplementary data associated with this article can be found in the online version at https://doi.org/10.1016/j.dib.2018.09.123.

References

[1] Liangrui He, Mi Fei, Jie Chen, Yunfei Tian, Yang Jiang, Yang Huang, Kai Xu, Juntao Hu, Zhi Zhao, Qiuhong Zhang, Haiyong Ni, Lei Chen, Graphitic C_3N_4 quantum dots for next-generation QLED display, Mater. Today (2018), https://doi.org/10.1016/j.mattod.2018.06.008 (in press).
[2] Y. Zhang, Q.W. Pan, G.Q. Chai, M.R. Liang, G.P. Dong, Q. Zhang, J. Qiu, Synthesis and luminescence mechanism of multicolor-emitting g-C_3N_4 nanopowders by low temperature thermal condensation of melamine, Sci. Rep. 3 (2013) 1943.
[3] S. Bayan, A. Midya, N. Gogurla, A. Singha, S.K. Ray, Origin of modified luminescence response in reduced graphitic carbon nitride nanosheets, J. Phys. Chem. C 121 (2017) 19383–19391.
[4] M. Rong, X. Song, T. Zhao, Q. Yao, Y. Wang, Xi Chen, Synthesis of highly fluorescent P,O-g-C_3N_4 nanodots for the label-free detection of Cu^{2+} and acetylcholinesterase activity, J. Mater. Chem. C 3 (2015) 10916–10924.
[5] Y. Zheng, Z. Zhang, C. Li, A comparison of graphitic carbon nitrides synthesized from different precursors through pyrolysis, J. Photochem. Photobiol. A 332 (2017) 32–44.
[6] P. Wu, J. Wang, J. Zhao, L. Guo, F.E. Osterloh, Structure defects in g-C_3N_4 limit visible light driven hydrogen evolution and photovoltage, J. Mater. Chem. A 2 (2014) 20338–20344.
[7] D. Das, S.L. Shinde, K.K. Nanda, Temperature-Dependent photoluminescence of g-C_3N_4: implication for temperature sensing, ACS Mater. Interfaces 8 (2016) 2181–2186.
[8] I. Papailias, T. Giannakopoulou, N. Todorova, D. Demotikali, T. Vaimakis, C. Trapalis, Effect of processing temperature on structure and photocatalytic properties of g-C_3N_4, Appl. Surf. Sci. 358 (2015) 278–286.